Strongly magnetized strange baryonic matter in neutron star

K. Miyazaki

E-mail: miyazakiro@rio.odn.ne.jp

Abstract

We investigate the strongly magnetized strange baryonic matter in a relativistic mean-field theory. We first take into account the hidden strange mesons and the field-dependent meson-baryon coupling constants. In low-density region the strongly magnetized neutron star (NS) matter is nearly iso-symmetric. The equation of state (EOS) therefore becomes softer than that of the normal NS matter. Because the magnetic field increases the threshold densities of Λ and Ξ^-, the EOS becomes stiffer in high-density region. However, the magnetic field has little effect on the effective masses of Λ and Σ. Taking into account the anomalous magnetic moments (AMMs) of baryons, the EOS becomes much stiffer although the threshold densities of Σ^+, Σ^0 and Ξ^0 decrease largely. The density dependence of the effective mass of Ξ precisely reflects the EOS while the effective masses of Λ and Σ are strongly influenced by the AMMs of nucleons through the scalar mean-field.

In recent astronomy and astrophysics there are great interests in the magnetars [1-5]. They are the neutron stars (NSs) that involve stronger magnetic fields $10^{14}G < B < 10^{15}G$ than the critical strength $B_C(e) = m_e/(2\mu_B) = 4.414 \times 10^{13}G$ for electrons. Although the field is still much weaker than the critical strength $B_C(N) = M_N/(2\mu_N) = 1.488 \times 10^{20}G$ for nucleons, the magnetar has stimulated the investigations [6-11] of extremely magnetized nuclear matter in a core of NS within the modern relativistic mean-field (RMF) theory [12]. In this respect, it is noted that in the RMF models the mass of a nucleon in dense medium is largely reduced from its free value, and so the magnetic field $B < B_C(N)$ is able to have significant effect on NS matter.

It is generally expected [13,14] that the hyperons play important roles in the inner cores of NSs. Most of the preceding works [6-11] for strongly magnetized NS matter however considered only nucleons as baryons. Only the paper [15] took into account hyperons within the so-called nonlinear Walecka (NLW) model [16]. On the other hand, it has been recently shown [17,18] that the NLW model is not useful in studying dense NS matter while the truly nonlinear RMF models, which should have field-dependent meson-baryon coupling constants, are promising. The most familiar RMF model embodying the true non-linearity is the Zimanyi-Moszkowski (ZM) model [19][1]. It has a renormalized

[1] Although Ref. [15] also calculated using the naive extension of the ZM model to hyperons, the results were not shown in figures.

$NN\sigma$ coupling constant by the renormalized nucleon mass M_N^*/M_N. However, its $NN\omega$ coupling constant is not renormalized and the renormalized mass $M_N^* = 0.85M_N$ is much larger than an appropriate value $M_N^* \simeq 0.6M_N$ [20,21] to reproduce the spin-orbit splitting of finite nuclei. Although an extension [22] of the ZM model has been recently developed, it has the same shortcoming as the ZM model and cannot be applied to dense strange baryonic matter in an unambiguous manner. To the contrary, the extended Zimanyi-Moszkowski (EZM) model developed in a series of papers [23-31] can reproduce the similar saturation property of nuclear matter to the Dirac-Brueckner-Hartree-Fock theory [32] and is applicable to strange baryonic matter in a unique manner because it is based on the constituent quark picture of baryons.

The purpose of this letter is to extend the investigation of Ref. [11], in which we developed the EZM model for the magnetized NS matter composed of only nucleons as baryons, so as to take into account hyperons. We also include the isovector scalar meson and the (hidden) strange mesons [33], which were not considered in Ref. [15].

Here we briefly review the strange baryonic matter in magnetic field B. The model Lagrangian in the mean-field approximation is

$$\begin{aligned}\mathcal{L} &= \sum_{\substack{b=p,n,\Lambda,\Sigma^+,\\ \Sigma^0,\Sigma^-,\Xi^0,\Xi^-}} \bar{\psi}_b \left(\not{p} - q_b \not{A} - \frac{1}{2}\kappa_b \, \sigma_{\mu\nu} F^{\mu\nu} - M_b^* - \gamma^0 V_b \right) \psi_b \\ &+ \sum_{l=e^-,\mu^-} \bar{\psi}_l \left(\not{p} + e\not{A} - m_l \right) \psi_l - \frac{1}{2}\, m_\sigma^2 \, \langle \sigma \rangle^2 - \frac{1}{2}\, m_\delta^2 \, \langle \delta_3 \rangle^2 - \frac{1}{2}\, m_{\sigma^*}^2 \, \langle \sigma^* \rangle^2 \\ &+ \frac{1}{2}\, m_\omega^2 \, \langle \omega_0 \rangle^2 + \frac{1}{2}\, m_\rho^2 \, \langle \rho_{03} \rangle^2 + \frac{1}{2}\, m_\phi^2 \, \langle \phi_0 \rangle^2 \,, \end{aligned} \tag{1}$$

where ψ_b and ψ_l are the Dirac fields of baryons and leptons. The charge and anomalous magnetic moment (AMM) [15] of each baryon are denoted by q_b and κ_b. The electromagnetic vector potential $A^\mu = (0, 0, xB, 0)$ is for the external magnetic filed B along the z-axis and $F^{\mu\nu} = \partial^\mu A^\nu - \partial^\nu A^\mu$. The isoscalar-scalar, isoscalar-vector, isovector-scalar and isovector-vector mean-fields are $\langle\sigma\rangle$, $\langle\omega_0\rangle$, $\langle\delta_3\rangle$ and $\langle\rho_{03}\rangle$, respectively. In addition we take into account the (hidden) scalar and vector strange-mesons σ^* and ϕ [33].

The effective mass M_b^* of a baryon b in baryonic matter is

$$M_b^* = m_b^* M_b = M_b + S_b. \tag{2}$$

The scalar potential S_b is given by

$$S_b = -g_{bb\sigma}^* \langle\sigma\rangle - g_{bb\delta}^* \langle\delta_3\rangle \, I_{3b} - g_{bb\sigma^*}^* \langle\sigma^*\rangle \,, \tag{3}$$

where $I_{3b} = (1, -1, 0, 1, 0, -1, 1, -1)$ for $b = (p, n, \Lambda, \Sigma^+, \Sigma^0, \Sigma^-, \Xi^0, \Xi^-)$ and $g_{bb\sigma}^*$ *etc.* are the renormalized scalar-meson coupling constants [28]. On the other hand, the vector

potential V_b is given by

$$V_b = g^*_{bb\omega} \langle \omega_0 \rangle + g^*_{bb\rho} \langle \rho_{03} \rangle I_{3b} + g^*_{bb\phi} \langle \phi_0 \rangle , \tag{4}$$

where $g^*_{bb\omega}$ *etc.* are the renormalized vector-meson coupling constants [28].

The energy density of matter is

$$\begin{aligned} \mathcal{E} &= \sum_{i=b,l} \varepsilon_i + \sum_b V_b \, \rho_b + \frac{1}{2} m_\sigma^2 \langle \sigma \rangle^2 + \frac{1}{2} m_\delta^2 \langle \delta_3 \rangle^2 + \frac{1}{2} m_{\sigma^*}^2 \langle \sigma^* \rangle^2 \\ &\quad - \frac{1}{2} m_\omega^2 \langle \omega_0 \rangle^2 - \frac{1}{2} m_\rho^2 \langle \rho_{03} \rangle^2 - \frac{1}{2} m_\phi^2 \langle \phi_0 \rangle^2 , \end{aligned} \tag{5}$$

where ρ_b is the baryon density in NS matter. The energy densities of charged baryon, neutral baryon, electron and muon are

$$\varepsilon_{b=p,\Sigma^+,\Sigma^-,\Xi^-} = \frac{\mu_N M_N B}{2\pi^2} \sum_{s=-1,1} \sum_{\nu}^{\nu_b^{\max}} \left\{ E_{Fb} k_{Fb}(\nu, s) + \left(\bar{M}_b(\nu, s) \right)^2 \ln \left| \frac{E_{Fb} + k_{Fb}(\nu, s)}{\bar{M}_b(\nu, s)} \right| \right\}, \tag{6}$$

$$\begin{aligned} \varepsilon_{b=n,\Lambda,\Sigma^0,\Xi^0} &= \frac{1}{4\pi^2} \sum_{s=-1,1} \left\{ \frac{1}{2} E_{Fb}^3 k_{Fb}(s) + \frac{2}{3} s \, \kappa_b B E_{Fb}^3 \left[\arcsin \frac{\bar{M}_b(s)}{E_{Fb}} - \frac{\pi}{2} \right] \right. \\ &\quad + \left. \left[\frac{1}{3} s \, \kappa_b B - \frac{1}{4} \bar{M}_b(s) \right] \left[\bar{M}_b(s) k_{Fb}(s) E_{Fb} + \left(\bar{M}_b(s) \right)^3 \ln \left| \frac{E_{Fb} + k_{Fb}(s)}{\bar{M}_b(s)} \right| \right] \right\}, \end{aligned} \tag{7}$$

$$\varepsilon_e = \frac{\mu_B m_e B}{2\pi^2} \sum_{\nu=0}^{\nu_e^{\max}} g(\nu) \left\{ E_{Fe} k_{Fe}(\nu) + \left(\bar{m}_e(\nu) \right)^2 \ln \left| \frac{E_{Fe} + k_{Fe}(\nu)}{\bar{m}_e(\nu)} \right| \right\}, \tag{8}$$

$$\varepsilon_\mu = \frac{\mu_\mu m_\mu B}{2\pi^2} \sum_{\nu=0}^{\nu_\mu^{\max}} g(\nu) \left\{ E_{F\mu} k_{F\mu}(\nu) + \left(\bar{m}_\mu(\nu) \right)^2 \ln \left| \frac{E_{F\mu} + k_{F\mu}(\nu)}{\bar{m}_\mu(\nu)} \right| \right\}, \tag{9}$$

where μ_N, μ_B and μ_μ are nuclear magneton, Bohr magneton and mu-magneton, respectively. The Landau quantum number ν in Eq. (6) starts from 1 for spin-up ($s = 1$) and 0 for spin-down ($s = -1$). The spin degenerate factor $g(\nu)$ in Eqs. (8) and (9) is 1 for $\nu = 0$ but 2 for $\nu \geq 1$. The Landau effective mass of each particle is defined as

$$\bar{M}_{b=p,\Sigma^+,\Sigma^-,\Xi^-}(\nu, s) = \left(M_b^{*2} + 4 \, \nu \mu_N M_N B \right)^{1/2} + s \, \kappa_b B, \tag{10}$$

$$\bar{M}_{b=n,\Lambda,\Sigma^0,\Xi^0}(s) = M_b^* + s \, \kappa_b B, \tag{11}$$

$$\bar{m}_e(\nu) = \left(m_e^2 + 4 \, \nu \mu_B m_e B \right)^{1/2}, \tag{12}$$

$$\bar{m}_\mu(\nu) = \left(m_\mu^2 + 4 \, \nu \mu_\mu m_\mu B \right)^{1/2}. \tag{13}$$

The Fermi energies are determined from the chemical potentials

$$E_{Fb} = \mu_b - V_b, \tag{14}$$

$$E_{Fl} = \mu_l. \tag{15}$$

(Do no confuse the magnetons with the chemical potentials.) The Fermi momentum of each particle on each Landau level is given by

$$k_{Fb}(\nu, s) = \left[E_{Fb}^2 - \left(\bar{M}_b(\nu, s)\right)^2\right]^{1/2} : \ b = p, \Sigma^+, \Sigma^-, \Xi^-, \tag{16}$$

$$k_{Fb}(s) = \left[E_{Fb}^2 - \left(\bar{M}_b(s)\right)^2\right]^{1/2} : \ b = n, \Lambda, \Sigma^0, \Xi^0, \tag{17}$$

$$k_{Fl}(\nu) = \left[E_{Fl}^2 - (\bar{m}_l(\nu))^2\right]^{1/2} : \ l = e^-, \mu^-. \tag{18}$$

The constraint that the Fermi momentum is a real value determines the maximum value $\nu_{b,l}^{\max}$ of the Landau quantum number for each particle.

The scalar-meson mean-fields are expressed by the renormalized masses M_p^*, M_n^* and M_Λ^*. Similarly, the vector-meson mean-fields are expressed by the vector potentials V_p, V_n and V_Λ. They are determined by extremizing the energy density (5). The resultant six nonlinear equations are formally same as Eqs. (44)-(49) in Ref. [34][2] although the baryon densities are given by

$$\rho_{b=p,\Sigma^+,\Sigma^-,\Xi^-} = \frac{\mu_N M_N B}{\pi^2} \sum_{s=-1,1} \sum_{\nu}^{\nu_b^{\max}} k_{Fb}(\nu, s), \tag{19}$$

$$\begin{aligned} \rho_{b=n,\Lambda,\Sigma^0,\Xi^0} &= \frac{1}{2\pi^2} \sum_{s=-1,1} \left\{ \frac{1}{3} \left(k_{Fb}(s)\right)^3 + \frac{1}{2}\, s\, \kappa_b B \left[\bar{M}_b(s) k_{Fb}(s) \right.\right. \\ &\quad \left.\left. + \ E_{Fb}^2 \left(\arcsin \frac{\bar{M}_b(s)}{E_{Fb}} - \frac{\pi}{2} \right) \right] \right\}, \end{aligned} \tag{20}$$

and the scalar densities are

$$\rho_{b=p,\Sigma^+,\Sigma^-,\Xi^-}^{(s)} = \frac{\mu_N M_b^* M_N B}{\pi^2} \sum_{s=-1,1} \sum_{\nu}^{\nu_b^{\max}} \frac{\bar{M}_b(\nu, s)}{\bar{M}_b(\nu, s) - s\kappa_b B} \ln \left| \frac{E_{Fb} + k_{Fb}(\nu, s)}{\bar{M}_b(\nu, s)} \right|, \tag{21}$$

$$\rho_{b=n,\Lambda,\Sigma^0,\Xi^0}^{(s)} = \frac{M_b^*}{4\pi^2} \sum_{s=-1,1} \left\{ E_{Fb} k_{Fb}(s) - \left(\bar{M}_b(s)\right)^2 \ln \left| \frac{E_{Fb} + k_{Fb}(s)}{\bar{M}_b(s)} \right| \right\}. \tag{22}$$

For the β-equilibrated NS matter, the six nonlinear equations are solved together with the baryon number conservation and the charge neutral condition under the β-equilibrium

[2] We mistyped the first terms in Eqs. (47) and (48) so that the nucleon mass M_N was missed.

condition using the 8-rank Newton-Raphson method so that we have the three independent effective masses and vector potentials and the bario- and electro-chemical potentials.

As has been shown in Refs. [8,9,11], only the extremely strong magnetic field $B > 10^{19}G$ is effective in the core of NS. In the present work we assume $B = 10^6 \times B_C\,(e)$ although it is stronger than the maximum magnetic field in NS expected from the scalar virial theorem [35]. The meson-baryon coupling constants are the same as those of the EZM-P in Ref. [34]. The AMMs of baryons are given in Table 1 of Ref. [15]. Figure 1 shows the pressures of cold β-equilibrated NS matter as functions of the total baryon density. The solid curve is for no magnetic field, and the dashed and dotted curves are for $B = 10^6 \times B_C\,(e)$ with and without taking into account the AMMs of baryons, respectively. Figures 2, 3 and 4 show the particle fractions in NS matter for $B = 0$ and $B = 10^6 \times B_C\,(e)$ without and with the AMMs.

In Fig. 1 the dashed and dotted curves are lower than the solid curve below $\rho_T = 0.34\text{fm}^{-3}$ and $\rho_T = 0.52\text{fm}^{-3}$, respectively. Especially, they have negative values below $\rho_T = 0.12\text{fm}^{-3}$ and $\rho_T = 0.20\text{fm}^{-3}$, respectively. The result is due to the fact [6,7] that the strongly magnetized NS matter is self-bound in low-density region as the normal nuclear matter is so. In fact, owing to the Landau quantization the protons in Figs. 3 and 4 are abundant even below $\rho_T = 0.3\text{fm}^{-3}$ in contrast to Fig. 2. The NS matter in the strong magnetic field is therefore nearly iso-symmetric. As a result, the electron is also abundant because of the charge neutral condition and so the threshold density of muon increases. To the contrary, below $\rho_T = 0.04\text{fm}^{-3}$ the magnetized NS matter becomes iso-asymmetric. There, the effects of the AMMs of nucleons are apparent. We find a proton rich matter in Fig. 3 but a neutron rich matter in Fig. 4.

There are noticeable kinks on the curves in Fig. 1 corresponding to the threshold densities of Λ. This is because in Figs. 2-4 the Ξ^-s appear just above Λ threshold and then the equations-of-state (EOSs) become much softer. The thresholds of Λ and Ξ^- in Fig. 3 are higher than those in Fig. 2. Therefore, above $\rho_T = 0.5\text{fm}^{-3}$ the EOS of the dotted curve is stiffer than the solid curve. Taking into account the AMMs, the threshold densities in Fig. 4 increase further. Consequently, the EOS of the dashed curve is the stiffest. On the other hand, the AMMs decrease the threshold densities of Σ^+, Σ^0 and Ξ^0 so largely as to be lower than those in Fig. 2 whereas Σ^- never appears in our calculation in spite of its negative charge. The results are due to the fact that Σ^+, Σ^0 and Ξ^0 have strong AMMs while Λ, Σ^- and Ξ^- have weak ones. For an example if $\kappa_{\Xi^0} = 0$ is assumed, the threshold density of Ξ^0 in Fig. 4 increases up to $\rho_T = 1.07\text{fm}^{-3}$.

Figure 5 shows the mass sequences of cold non-rotating NSs by integrating the Tolman-Oppenheimer-Volkov equation [36]. For the crust of NS we employ the EOSs by Feynman-Metropolis-Teller, Baym-Pethick-Sutherland and Negele-Vautherin in Ref. [37]. It is noted that they are for zero magnetic field and so are not appropriate for the strongly magnetized NS. Nevertheless, we simply interpolate between the EOS of Negele-Vautherin below $\rho_T = 0.1\text{fm}^{-3}$ and the EOSs of the dashed and dotted curve in Fig. 1 above

$\rho_T = 0.12\text{fm}^{-3}$ and $\rho_T = 0.20\text{fm}^{-3}$. It is also noted that we consider the contribution to EOS only from matter but not from magnetic field. Consequently, the dashed and dotted curves in Fig. 5 do not describe real NSs. In this respect, even an effort of Ref. [38] is not sufficient for studying the strongly magnetized NSs. This is because the RMF model of NS matter assumes the spherical symmetry while the external magnetic field requires the axial symmetry on the Einstein equation. The strongly polarized nuclear matter within the relativistic theory [39,40] is beyond the mean-field approximation. Moreover, there is a problem [41] on the stability of axisymmetric NS matter. However, the results in Fig. 5 are sufficient for our purpose to show the effects of strong magnetic field and the AMMs of baryons. In fact, we find the remarkable differences in the mass and radius of NSs. The most massive NS for zero magnetic field has a gravitational mass $M_G = 1.566M_\odot$ and a radius $R = 13.11$km while that in the strong magnetic field has $M_G = 1.634M_\odot$ and $R = 10.65$km. The small radius in the latter is due to the softest EOS of the dotted curve in Fig. 1 at low densities. To the contrary, the effect of the AMMs produces much larger mass $M_G = 3.198M_\odot$ and radius $R = 15.19$km because of the stiffest EOS of the dashed curve in Fig. 1 at high densities.

Figure 6 shows the effective masses of proton as functions of the total baryon density. As the proton is abundant, the σ mean-field becomes strong and m_p^* becomes small. The dotted curve, which is lower than the solid curve over whole range of density, therefore reflects the abundant proton in Fig. 3 relative to Fig. 2. On the other hand, the difference between the solid and dashed curves precisely reflects the corresponding EOSs in Fig. 1. This is understood from the Gibbs-Duhem relation $P = \mu_n\rho_T - \mathcal{E}$, which indicates that a weaker σ mean-field or a larger m_p^* leads to a stiffer EOS. Figure 7 shows the effective mass of Ξ^-. It reflects the effect of σ^* mean-field because Ξ has the largest strangeness $S = -2$. Above the threshold densities of Λ, which are seen as kinks on the curves, the hyperons are abundant and so the σ^* mean-field is strong. A stronger σ^* mean-field leads to a smaller $m_{\Xi^-}^*$. From the Gibbs-Duhem relation, a smaller $m_{\Xi^-}^*$ means a softer EOS. The curves in Fig. 7 are therefore consistent to the corresponding EOSs in Fig. 1. The result of $m_{\Xi^0}^*$ is similar to $m_{\Xi^-}^*$ although it has not been shown in figure. To the contrary, for m_Λ^* and $m_{\Sigma^-}^*$ in Figs. 8 and 9 the kinks on the solid curves at Λ thresholds are not noticeable and the differences between the solid and dotted curves are small. After taking into account the AMMs, the kinks and the effects of the magnetic field on the effective masses are apparent. The results seem to be remarkable because the AMMs of Λ and Σ^- are weak. However, they are not the direct results of the AMMs of Λ and Σ^- themselves but the indirect results of the strong AMMs of nucleons through the σ mean-field. In fact, the results of Σ^+ and Σ^0, which have strong AMMs, are similar to $m_{\Sigma^-}^*$ although they have not been shown in figures.

We have investigated the strongly magnetized NS matter composed of all the baryon octets within the extended Zimanyi-Moszkowski model. The new ingredients in this work are the isovector scalar mean-field, the contributions of strange mesons and the

field-dependent meson-baryon coupling constants. We have assumed extremely strong magnetic field $B = 4.414 \times 10^{19} G$. In low-density region the strongly magnetized NS matter is nearly iso-symmetric. The EOS therefore becomes softer than that of the normal NS matter. In NS mass sequence, the softness of the EOS is reflected in a small radius of the most massive NS. However, the magnetic field has little effect on the effective masses of Λ and Σ. Taking into account the AMMs of baryons, the EOS of the strongly magnetized NS matter becomes much stiffer although the threshold densities of Σ^+, Σ^0 and Ξ^0 decrease largely. The mass and radius of the most massive NS are therefore much larger than those of the observed NSs. The dependence of Ξ effective mass on the total baryon density reflects the EOS precisely while the effective masses of Λ and Σ are strongly influenced by the AMMs of nucleons through the σ mean-field.

Recently, we have shown [42] that the antikaon condensation has a significant effect on the EOS of normal NS matter. Although Ref. [43] has already investigated the antikaon in magnetized NS matter, it considers only nucleons as baryons. In a future work we will extend the present investigation to take into account the antikaon condensation.

References

[1] R.C. Duncan, arXiv:astro-ph/0002442.

[2] C. Kouveliotou, R.C. Duncan and C. Thompson, Scientific American, February 2003.

[3] P.M. Woods and C. Thompson, *Compact Stellar X-ray Sources*, Ch. 14, ed. W.H.G. Lewin and M. van der Klis (Cambridge University Press, Cambridge, 2004) [arXiv:astro-ph/0406133].

[4] J.S. Heyl, "Magnetars" in *Proc. of 22nd Texas Symposium on Relativistic Astrophysics at Stanford University*, Stanford, 2004, ed. P. Chen et al. [http://www.slac.stanford.edu/econf/C041213/].

[5] A.K. Harding, D. Lai, arXiv:astro-ph/0606674.

[6] S. Chakrabarty, D. Bandyopadhyay and S. Pal, Phys. Rev. Lett. **78** (1997) 2898 [arXiv:astro-ph/9703034].

[7] Y.F. Yuan and J.L. Zhang, Astrophys. J. **525** (1999) 950.

[8] A. Broderick, M. Prakash and J.M. Lattimer, Astrophys. J. **537** (2000) 351.

[9] G. Mao, N.V. Kondratyev, A. Iwamoto, Z. Li, X. Wu, W. Geiner and N.I. Mikhailov, Chin. Phys. Lett. **20** (2003) 1238 [arXiv:astro-ph/0111374].

[10] F.X. Wei, G.J. Mao, C.M. Ko, L.S. Kisslinger, H. Stöcker and W. Greiner, J. Phys. G **32** (2006) 47 [arXiv:nucle-th/0508065].

[11] K. Miyazaki, Mathematical Physics Preprint Archive (mp_arc) 06-39.

[12] B.D. Serot and J.D. Walecka, *Advances in Nuclear Physics*, Vol. **16** (Plenum, New York, 1986).

[13] S. Balberg, I. Lichtenstadt and G.B. Cook, Astrophys. J. Suppl. **121** (1999) 515

[14] F. Weber, J. Phys. G **27** (2001) 465 [arXiv:astro-ph/0008376]; F. Weber, A.T. Cuadrat, A. Ho and P. Rosenfield, arXiv:astro-ph/0602047.

[15] A.E. Broderick, M. Prakash and J.M. Lattimer, Phys. Lett. B **531** (2002) 167 [arXiv:astro-ph/0111516].

[16] N.K. Glendenning and S.A. Moszkowski, Phys. Rev. Lett. **67** (1991) 241.

[17] T. Klähn, *et al.*, arXiv:nucl-th/0602038.

[18] K. Miyazaki, Mathematical Physics Preprint Archive (mp_arc) 06-103.

[19] J. Zimanyi and S.A. Moszkowski, Phys. Rev. C **42** (1990) 1416.

[20] W. Koepf, M.M. Sharma and P. Ring, Nucl. Phys. A **533** (1991) 95.

[21] M.M. Sharma, M.A. Nagarajan and P. Ring, Ann. of Phys. **231** (1994) 110.

[22] E.E. Kolomeitsev and D.N. Voskresensky, Nucl. Phys. A **759** (2005) 373 [arXiv:nucl-th/0410063].

[23] K. Miyazaki, Mathematical Physics Preprint Archive (mp_arc) 05-178.

[24] K. Miyazaki, Mathematical Physics Preprint Archive (mp_arc) 05-190.

[25] K. Miyazaki, Mathematical Physics Preprint Archive (mp_arc) 05-199.

[26] K. Miyazaki, Mathematical Physics Preprint Archive (mp_arc) 05-206.

[27] K. Miyazaki, Mathematical Physics Preprint Archive (mp_arc) 05-216.

[28] K. Miyazaki, Mathematical Physics Preprint Archive (mp_arc) 05-224.

[29] K. Miyazaki, Mathematical Physics Preprint Archive (mp_arc) 05-233.

[30] K. Miyazaki, Mathematical Physics Preprint Archive (mp_arc) 06-91.

[31] K. Miyazaki, Mathematical Physics Preprint Archive (mp_arc) 05-427.

[32] R. Brockmann and R. Machleidt, Phys. Rev. C **42** (1990) 1965.

[33] J. Schaffner, C.B. Dover, A. Gal, C. Greiner and H. Stőker, Phys. Rev. Lett. **71** (1993) 1328.

[34] K. Miyazaki, Mathematical Physics Preprint Archive (mp_arc) 06-175.

[35] D. Lai and S.L. Shapiro, Astrophys. J. **383** (1991) 745.

[36] W.D. Arnett and R.L. Bowers, Astrophys. J. Suppl. **33** (1977) 415.

[37] V. Canuto, Ann. Rev. Astr. Ap. **12** (1974) 167; **13** (1975) 335.

[38] C.Y. Cardall, M. Prakash and J.M. Lattimer, Astrophys. J. **554** (2001) 322.

[39] T. Maruyama and T. Tatsumi, Nucl. Phys. A **693** (2001) 710 [arXiv:nucl-th/0010018].

[40] P.G. Krastev and F. Sammarruca, arXiv:nucl-th/0607029.

[41] A.P. Martínez, H.P. Rojas and H.J.M. Cuesta, Eur. Phys. J. C **29** (2003) 111 [arXiv:astro-ph/0303213].

[42] K. Miyazaki, Mathematical Physics Preprint Archive (mp_arc) 06-192.

[43] P. Dey, A. Bhattacharyya and D. Bandyopadhyay, J. Phys. G **28** (2002) 2179 [arXiv:astro-ph/0209100].

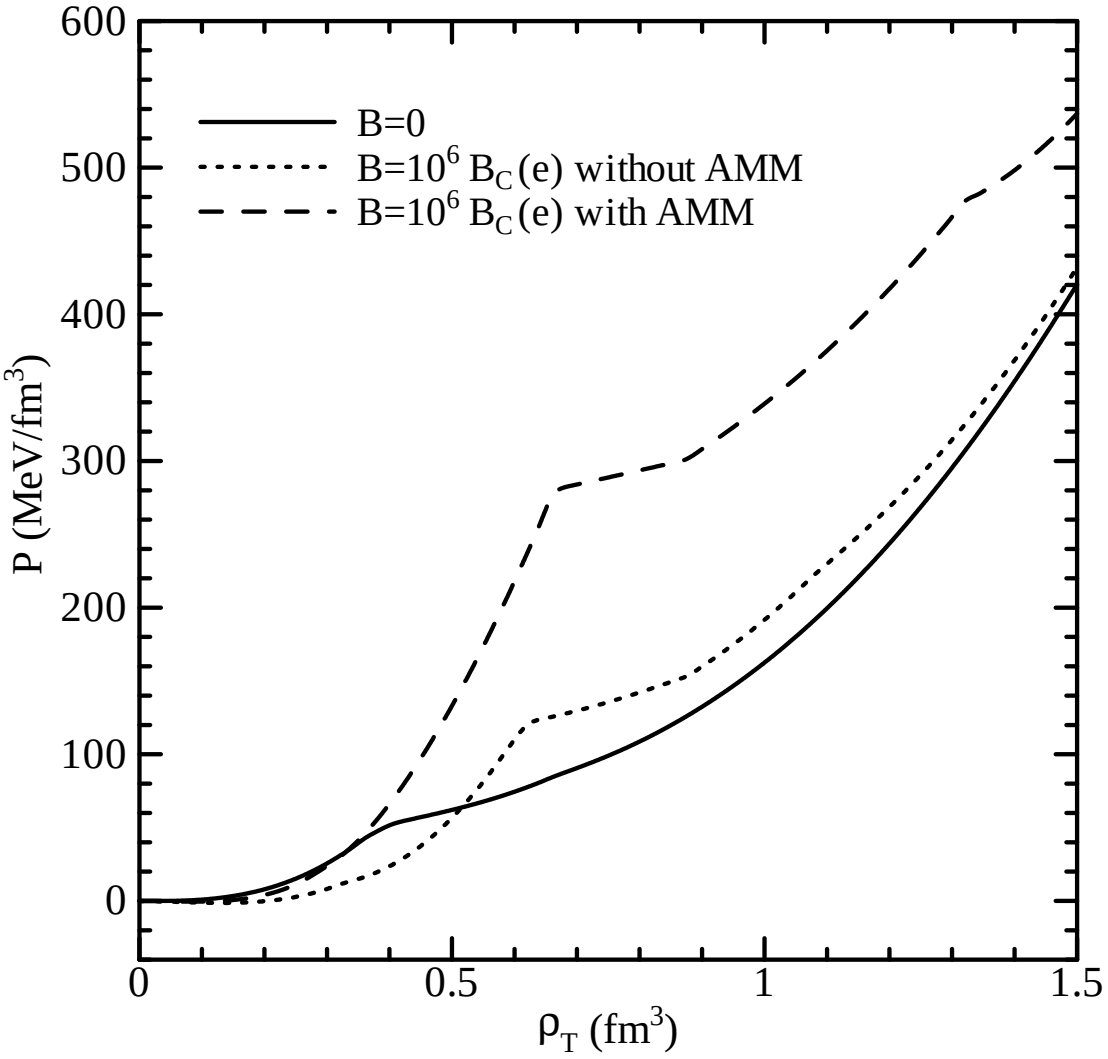

Figure 1: The pressures of cold β-equilibrated NS matter as functions of the total baryon density. The solid curve is for no magnetic field while the dashed and dotted curves are for $B = 10^6 \times B_C\,(e)$ with and without taking into account the AMMs of baryons, respectively.

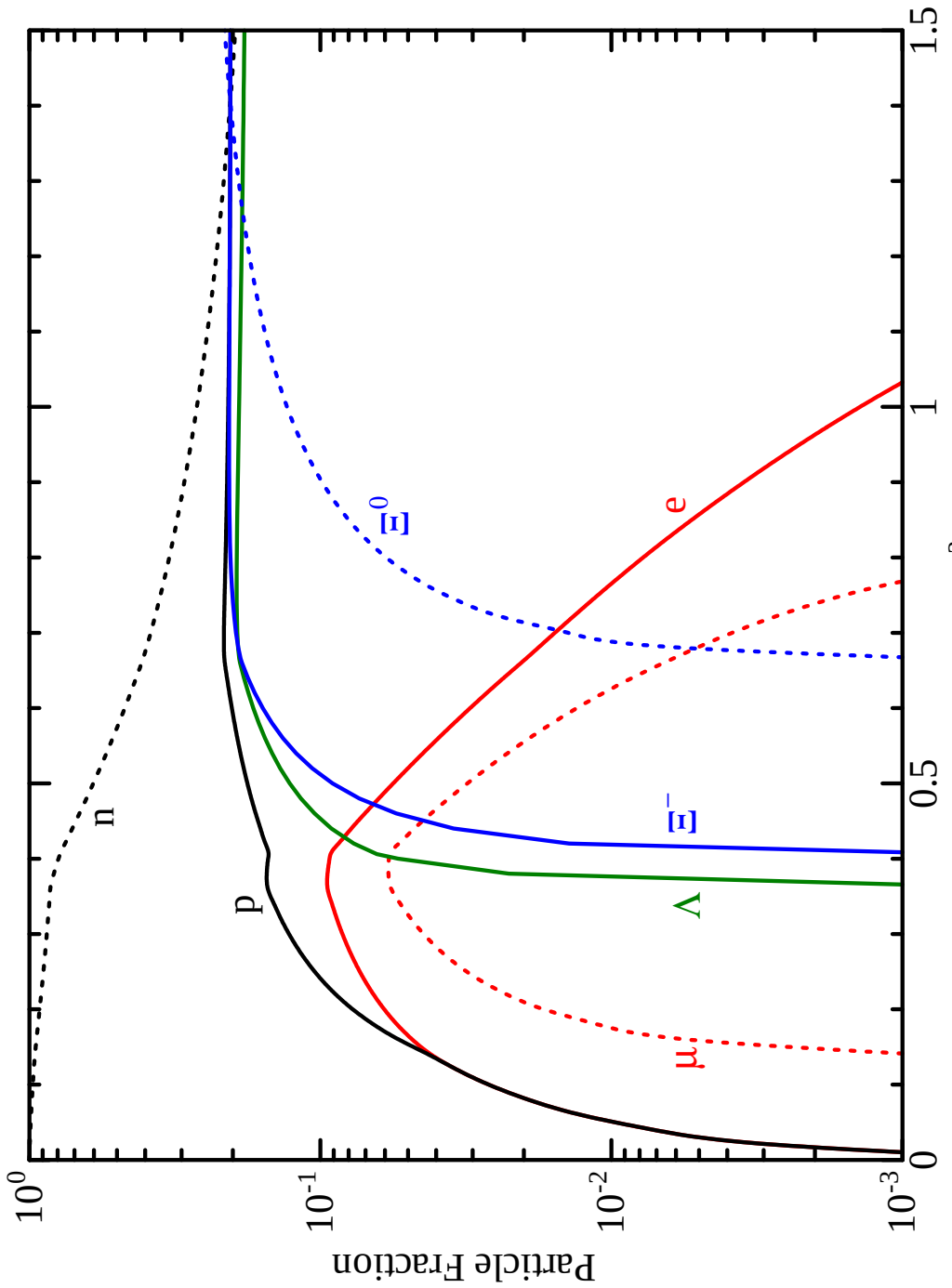

Figure 2: The particle fractions in cold β-equilibrated NS matter for $B = 0$.

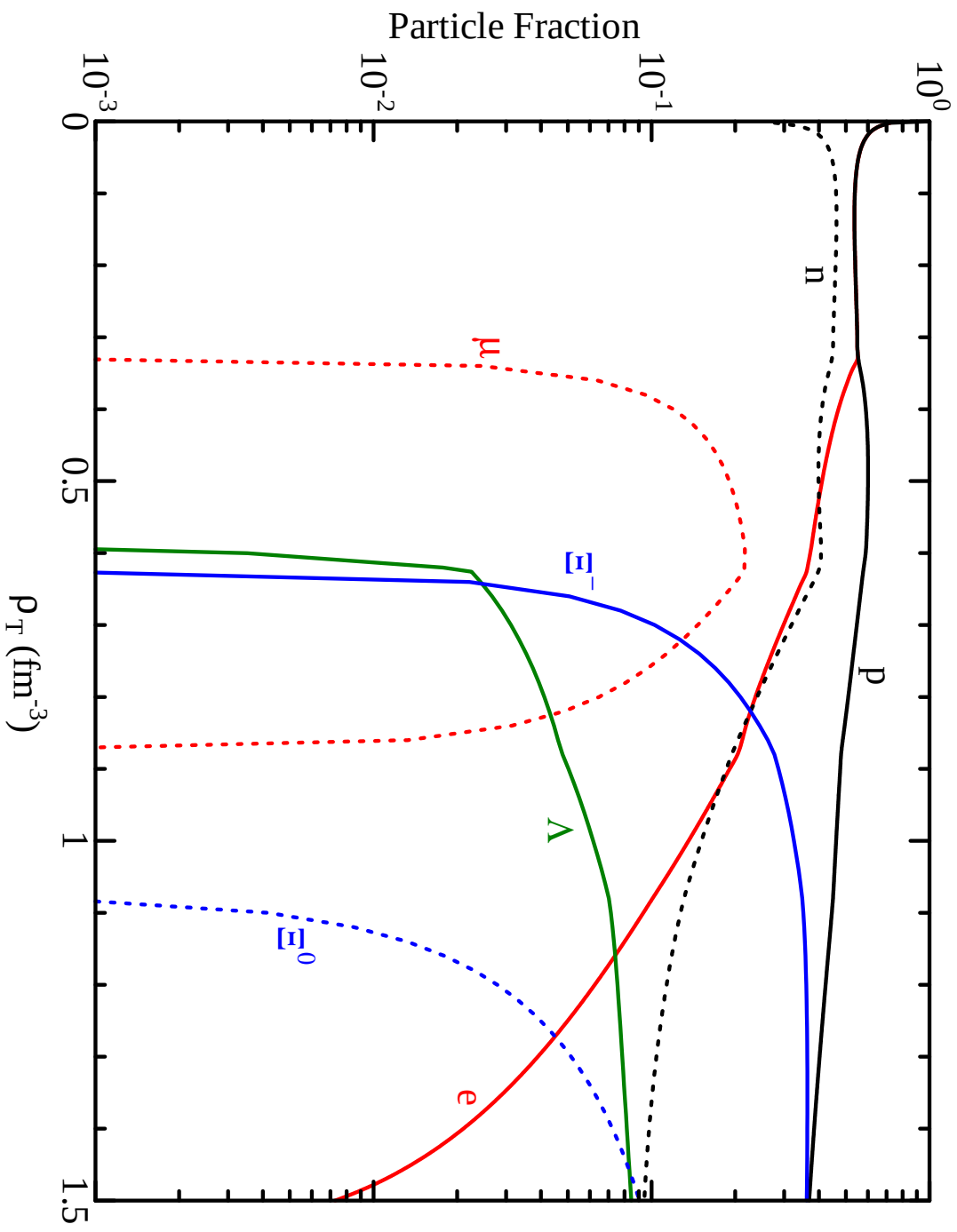

Figure 3: The particle fractions in cold β-equilibrated NS matter for $B = 10^6 \times B_c(e)$ without taking into account the AMMs of baryons.

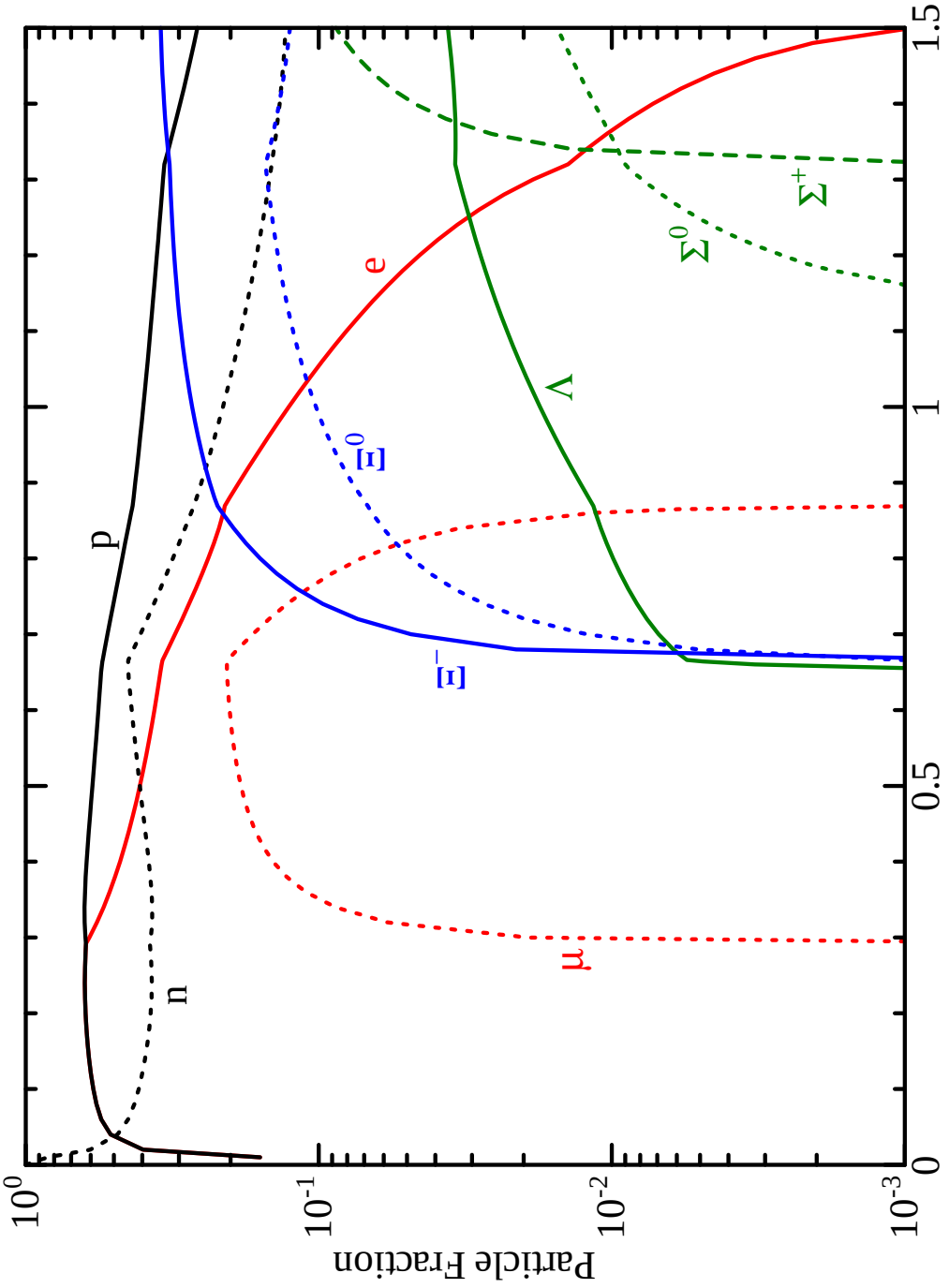

Figure 4: The same as Fig. 3 but taking into account the AMMs.

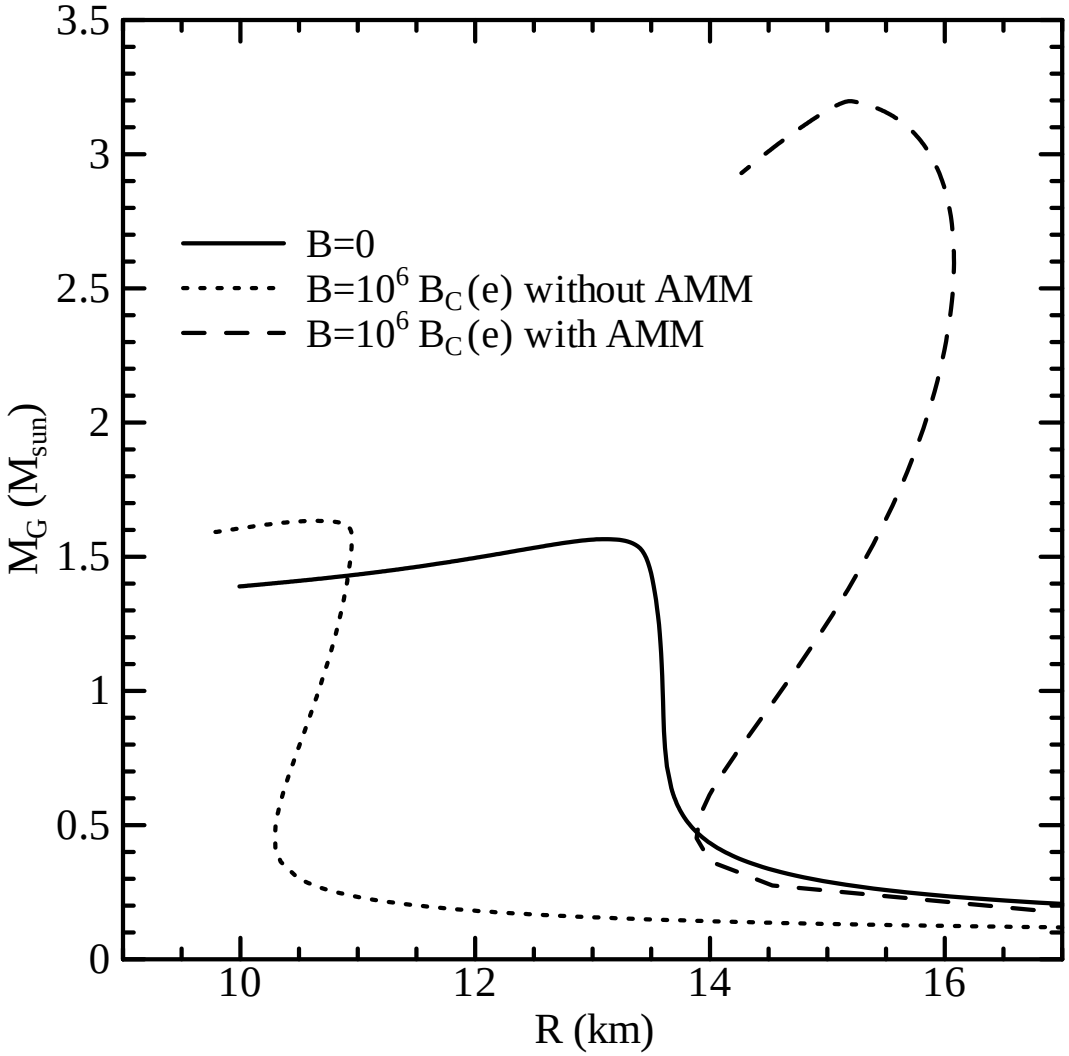

Figure 5: The mass sequences of cold non-rotating NS. The curves are the same as Fig. 1.

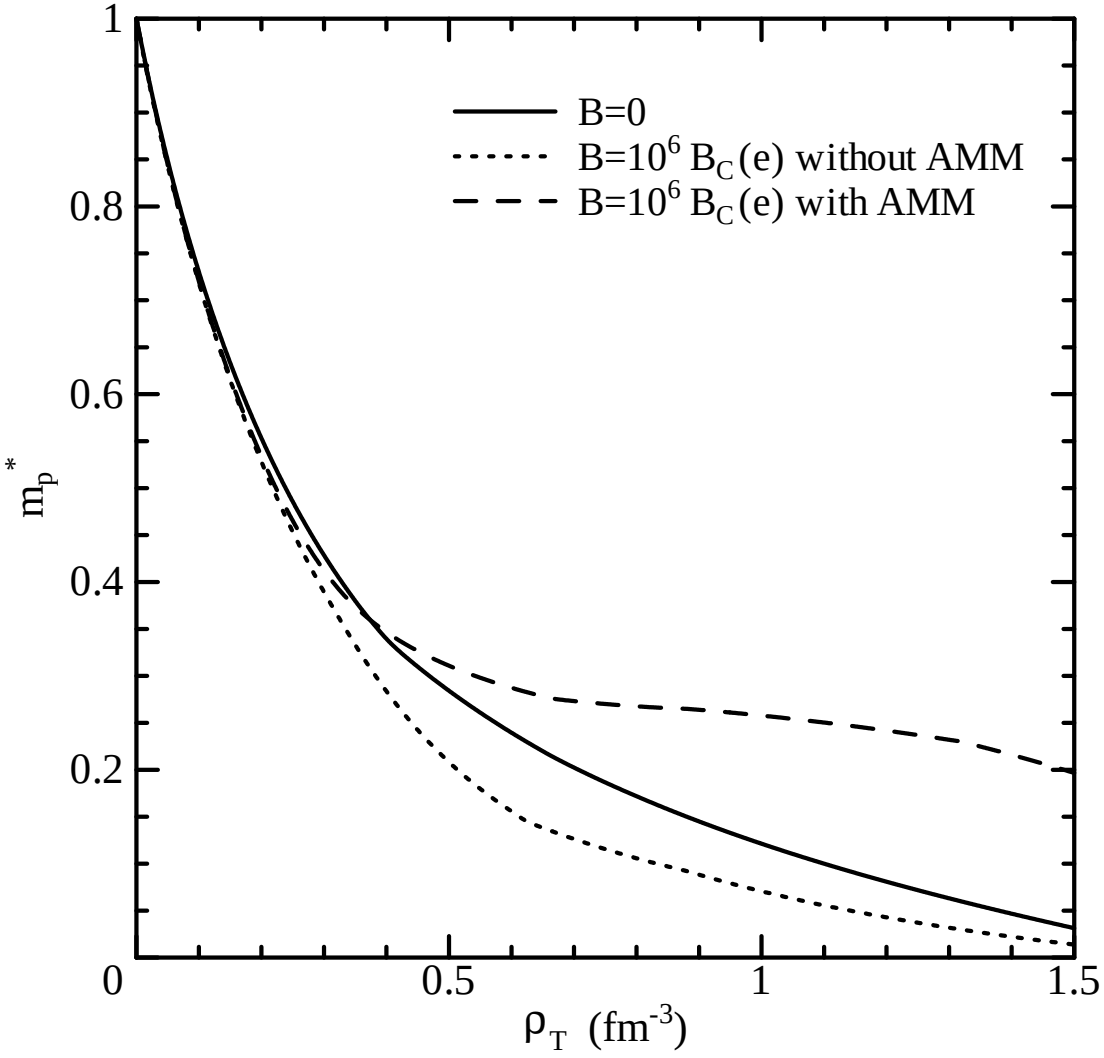

Figure 6: The effective masses of proton in NS matter as functions of the total baryon density. The curves are the same as Fig. 1.

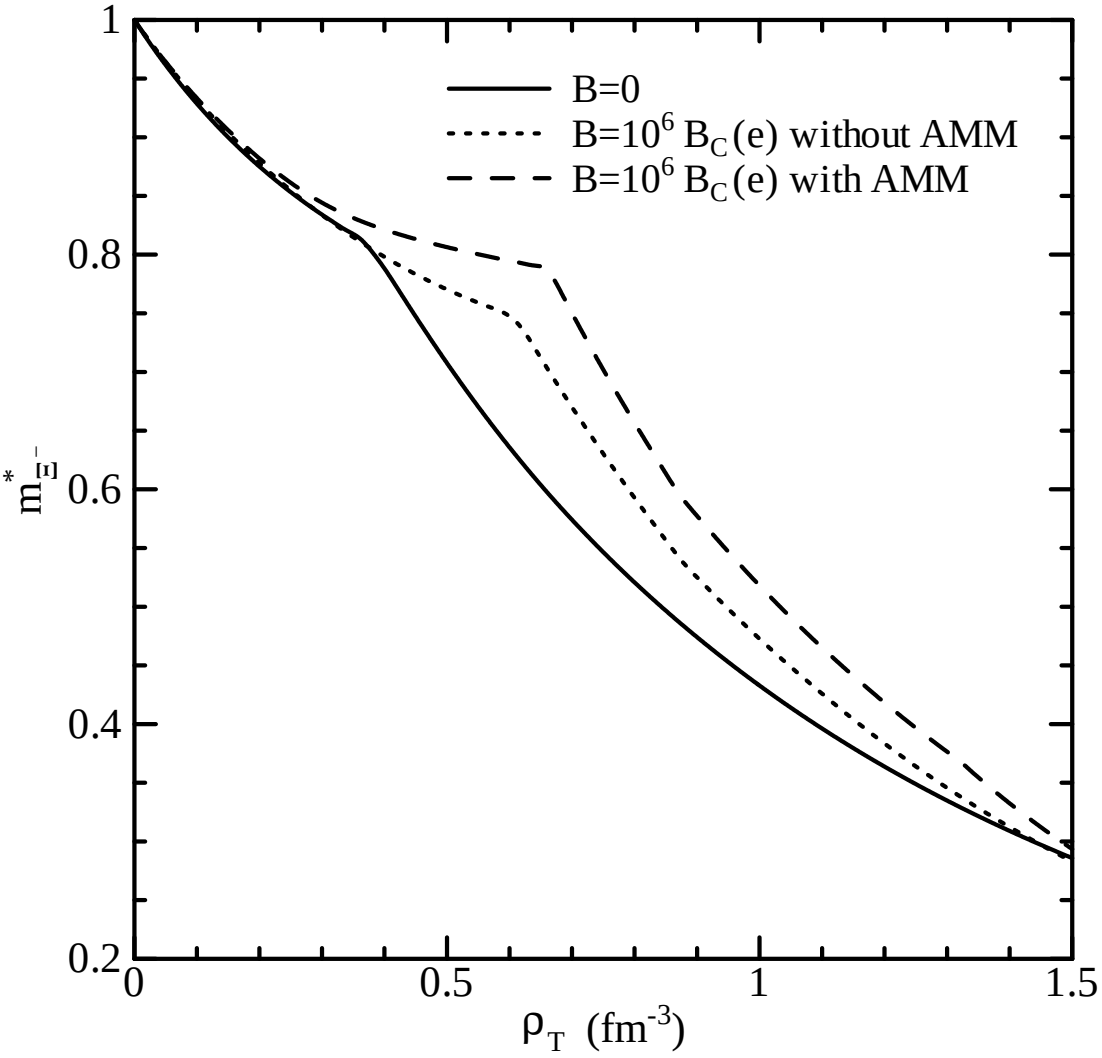

Figure 7: The same as Fig. 6 but for Ξ^-.

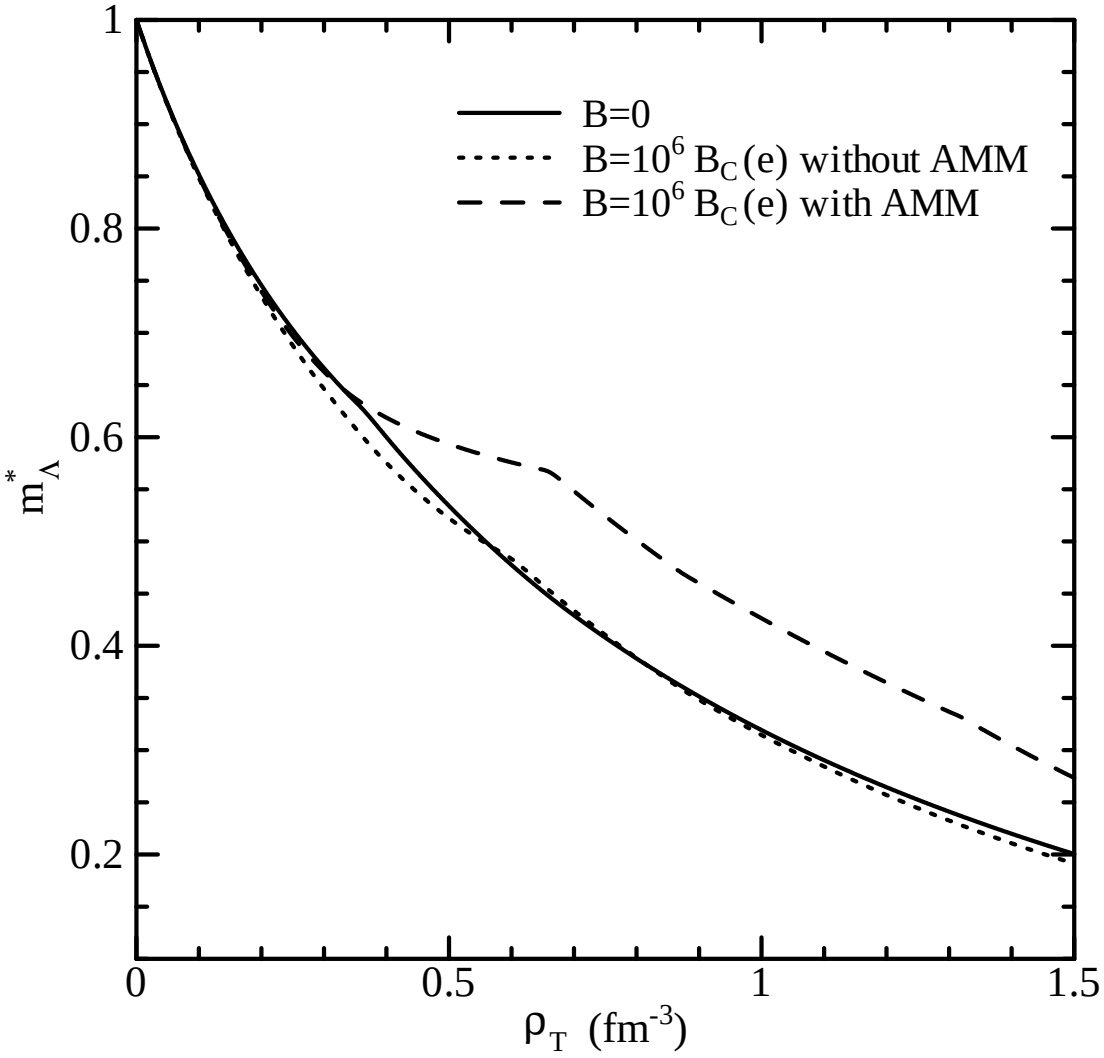

Figure 8: The same as Fig. 6 but for Λ.

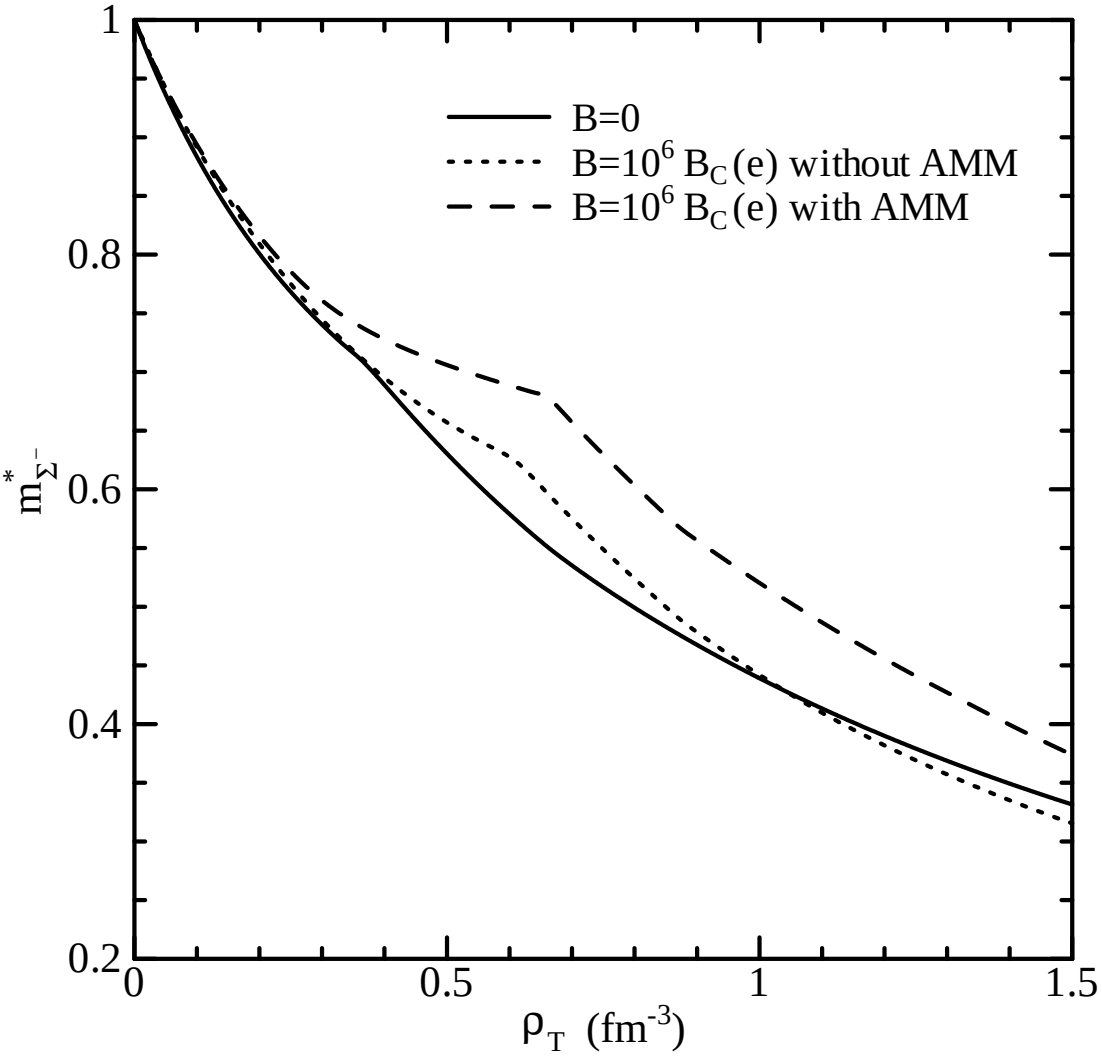

Figure 9: The same as Fig. 6 but for Σ^-.